平 成 ２ ５ 年 度

京 都 大 学 大 学 院 理 学 研 究 科

Ｄ Ｃ ３ 回 生 研 究 発 表 会
要旨集

２０１４年1月２０日（月）

物 理 学 第 一 分 野

物理学第一分野ＤＣ３回生研究発表会

場所：理学研究科５号館　５階・第四講義室
発表：１５分（別に質問１０分程度）

２０１４年1月２０日（月）９：００～　開始

目　　次

１０：４０～１０：５０　休憩

１２：０５～１３：３０　昼休み

１５：１０～１５：２０　休憩

１７：００～１７：１０　休憩

The kinetic theory of lane formation

Advanced statistical dynamics group　Masahiro Ikeda

Abstract We investigate pattern dynamics of a two-dimensional oppositely driven binary particle system. A surprisingly rich dynamical behavior including lane formation, jamming, oscillation and turbulence-like dynamics is found using extensive particle-based simulations. We also develop the kinetic theory based on Enskog equation to describe the lane formation process.

Lane formation is one of the representative examples of nonequilibrium phase transitions. When two kinds of particles are driven in opposite directions, the system exhibits a self-organization from a uniformly mixed state into strongly ordered anisotropic patterns. This driven segregation phenomenon, first found in the computer simulations [1], has been observed in laboratory experiments such as mixtures of oppositely charged colloids [2]. Another important class of examples is pedestrian and traffic flow dynamics. By tracing single-particle motions in colloidal dispersions, a recent paper suggested that the lane formation takes place due to a "lock-in" mechanism [3]. The mobility of particles is initially isotropic by frequent collisions, which, however, decreases considerably once the lane is formed. This microscopic dynamics leads to the trapping of particles within the lanes and thus to the growth of the lane structures. This is also consistent with a physical picture employed in the phenomenological dynamic density-functional theory [4].

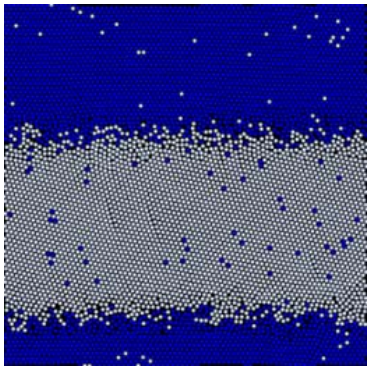

Fig. 1.
The lane formation observed in the particle-based simulations

We show the instability of the lane formation observed by our simulation of a particle-based model in which the self-propelling elements interact frictionally with the substrate [5]. A typical snapshot of the lane formation in this simulation is shown in Fig. 1.

We also develop the kinetic theory based on Enskog equation [6] to describe the lane formation process for the counter driven dissipative particles. We have derived a set of hydrodynamic equations for the density, the momentum current, and the kinetic temperature for a binary mixture for the counter driven particles. We also characterize the interface between two stable phases of driven particles. Such a microscopic derivation of the driven particles is quite new, and thus, the derived equations are completely different from the conventional hydrodynamic equations.

We also try to discuss the instability for the straight interface between two phases in terms of hydrodynamic equations derived from the kinetic theory. This research enables us to understand the mechanism of various phenomena observed in our former numerical study of the lane formation.

References

[1] J. Dzubiella, G. P. Hoffmann, and H. Löwen, Phys. Rev. E **65**, 021402 (2002).
[2] Mirjam E. Leunissen, et al, Nature **437** 235 - 240 (2005).
[3] Teun Vissers, Adam Wysocki, et al, Soft Matter, **7**, 2352 (2011).
[4] J. Chakrabarti, J. Dzubiella and H. Löwen, Europhys. Lett. **61** 415 (2003).
[5] M. Ikeda, H. Wada and H. Hayakawa, EPL **99**, 68005 (2012).
[6] V. Garzó and J. W. Dufty, Phys. Rev. E **59**, 5895 (1999).

Non-Equilibrium Quantum Spin Transport Theory Based on Schwinger-Keldysh Formalism

Physics of Matter: Condensed Matter Physics (YITP) Kouki Nakata

Abstract We microscopically investigate the non-equilibrium quantum transport phenomena of magnetization on the basis of the Schwinger-Keldysh formalism. In particular, we clarify the microscopic mechanism for the generation of the spin currents in metals and insulators and construct the theories.

Owing to the indirect measurement by using the inverse spin-Hall effects [1], the spin current, which had been simply the theoretical concept for a long time, was qualified as the physical quantity. Consequently, a new branch of physics called spintronics, whose central theme is the manipulation of spin degrees of freedom as well as charge ones of electrons, has seen a rapid development over the last decades. Then, establishing the methods for the generation of the spin currents and constructing the microscopic theory have become the significant issues from viewpoints of both fundamental science and applications to information and communication technologies.

First, we reformulate the spin pumping theory on the basis of the Schwinger-Keldysh formalism, which can explicitly treat the system out of equilibrium at finite temperatures, and construct the microscopic quantum spin pumping theory [2]. Spin pumping is the experimentally established method [1] for the generation of the spin currents and the spin pumping system is defined as the junction between the non-magnetic metal and the ferromagnet. Although the spin pumping phenomenon is well understood at the level of the semi-classical theory [3], to microscopically describe the phenomenon has been an urgent issue. To obtain the understanding of spin pumping beyond the semi-classical regime, on the basis of the spin continuity equation of the conduction electrons, we microscopically describe the non-equilibrium spin-flip process arising from quantum effects at the interface, where the exchange interaction between the conduction electrons and the magnons works. Consequently, we clarify that spin pumping is characterized by the spin relaxation torque (SRT), which breaks the spin conservation law of the conduction electrons, and find that all information about the spin-flip processes and the applied microwave are captured by the SRT. Then, the net pumped spin current, which can be regarded as the non-linear response to the applied microwaves, is represented only in terms of the SRT. The distinction between our quantum theory and the preceding semi-classical one is also clarified. In addition, we theoretically predict that spin pumping is generated also by the electron spin resonance as well as the usual method via the ferromagnetic resonance. This theoretical prediction is the important milestone to show the validity of our quantum theory.

After that, motivated by the breakthrough of the experimental techniques using the microwave pumping method [4], we show that the quasi-equilibrium Bose-Einstein condensation (BEC) of magnons occurs also in the spin-pumping systems. To this aim, we construct a theory on the quasi-equilibrium magnon BEC where the thermalization processes, which work as a bridge between the magnon pumping driven by microwaves and the resultant magnon BEC, are phenomenologically taken into account. Magnon BEC is a macroscopic state with quantum coherence and is robust against the loss of information. On top of this, remarkably, the quasi-equilibrium magnon BEC can be experimentally produced at room temperature by using the microwave pumping method. Thus, we can make a bridge between the research on spintronics and magnon BEC and theoretically open a new door to experimentally exploring the spin current in the ferromagnetic insulators.

References

[1] E. Saitoh et al., Appl. Phys. Lett., **88** (2006) 182509.
[2] K. Nakata, J. Phys. Soc. Jpn., **81** (2012) 064717., K. Nakata, J. Phys.: Condens. Matter., **25** (2013) 116005.
[3] Y. Tserkovnyak et al., Rev. Mod. Phys., 77 (2005) 1375.
[4] S. O. Demokritov et al., Nature, **443** (2006) 430.

Effect of Elastic Vibrations on Normal Head on Collisions of Isothermal Spheres

Advanced statistical dynamics group Ryo Murakami

From the simulation of elastic sphere collisions, we find that the restitution coefficient e oscillates against the impact speed due to the collision-vibration resonance. We also find a sinusoidal behavior of e against the initial phase in the eigenmodes for the collision of thermally activated spheres, which results in $e > 1$.

The impact processes play important roles in various fields ranging from granular physics to nanoscience. The main aim of the research on impact processes is to know the loss of the translational energy during the collision, which is characterized by the restitution coefficient e, the ratio of the rebound speed to the impact speed. There are three known mechanisms for the loss of the translational energy, which causes e to be less than unity: (1) the excitation of vibration in the colliding object, (2) energy dissipation due to the solid viscosity in the object, and (3) energy loss due to a plastic deformation or fracture of the object [1]. Many papers (e.g. [2, 3]) dealed with the mechanism (2) by applying the quasi-static theory in which the mechanism (1) is ignored. References. [4, 5] investigated the mechanism (1) using two dimensional elastic disks. Here I address both the mechanisms (1) and (2) by using a model of isothermal visco-elastic spheres which is the natural extension of the previous 2D model [4, 5]. In particular, I focus on the mechanism (1), and reveal the role of excited elastic vibrations during collisions. Thus, I restrict my interest to slow impacts, and ignore the mechanism (3) in the presentation.

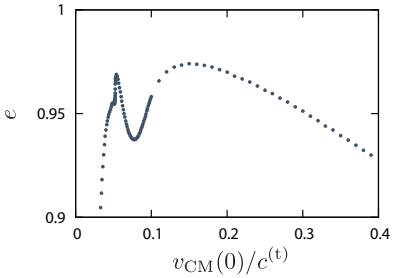

Figure 1: $v_{\rm CM}$ dependence of e.

Figure 1 shows the impact speed $v_{\rm CM}$ dependence of e, where $c^{(\rm t)}$ is the transverse sound speed for the sphere [6]. I find a characteristic oscillation of $e(v_{\rm CM})$ which has never reported even in Refs. [4, 5]. From the detailed analysis, I confirm that this behavior arises from the resonance between the duration of contact and the oscillation period of vibration of each mode [6].

There exists "super rebound" characterized by $e > 1$ for slow impacts between nanoclusters at finite temperature [7]. Motivated by this findings, I investigate the collision between a thermally activated sphere and a flat wall. In the super rebounds, a part of thermal energy is transferred into the translational energy, which seems to violate the second law of thermodynamics. However, Tasaki [8] indicated that super rebounds do not conflict with the second law for impact processes, and the probability of the restitution coefficient satisfies an extended fluctuation theorem. In the presentation, I numerically verify the extended fluctuation theorem.

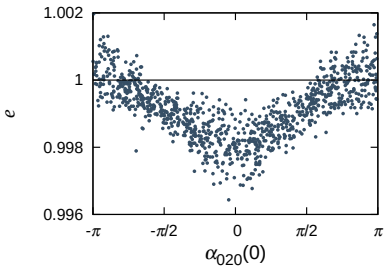

Figure 2: $\alpha_{020}(0)$ dependence of e.

Figure 2 shows e against the initial phase of the quadrupole mode $\alpha_{020}(0)$ for $v_{\rm CM}(0) = 0.007c^{(\rm t)}$ and the temperature $T = 2.14 \times 10^{-8} M(c^{(\rm t)})^2$ (300 K in the physical unit) [6]. I find that a sinusoidal behavior of $e(\alpha_{020}(0))$ is responsible for super rebounds if $v_{\rm CM}(0)$ is nearly equal to or slower than the thermal speed. I reproduce the sinusoidal behavior from the perturbation theory of this system, and find that the restitution coefficient can exceed unity if the sphere expands to the axial direction at the instant of the impact.

References

[1] K. L. Johnson, *Contact Mechanics* (Cambridge University Press, 1985).

[2] G. Kuwabara and K. Kono, Jpn. J. Appl. Phys. **26**, 1230 (1987).

[3] N. V. Brilliantov, F. Spahn, J.-M. Hertzsch, and T. Pöschel, Phys. Rev. E **53**, 5382 (1996).

[4] F. Gerl and A. Zippelius, Phys. Rev. E **59**, 2361 (1999).

[5] H. Hayakawa and H. Kuninaka, Chem. Eng. Sci. **57**, 239 (2002).

[6] R. Murakami and H. Hayakawa, submitted to Phys. Rev. E (arXiv:1309.095474).

[7] H. Kuninaka and H. Hayakawa, Phys. Rev. E **79**, 031309 (2009).

[8] H. Tasaki, in *The proceedings of the RIMS workshop "Micro-Macro Duality in Quantum Analysis"*, p. 102, Japan, 2006, No. 1507, RIMS, Kyoto University.

Superconducting properties of heavy fermion thin films and superlattices

Electronic properties of solids laboratory Masaaki Shimozawa

Abstract We fabricate a new type of heavy fermion superconducting superlattices with thickness modulations. We find that the modulations result in drastic changes of the upper critical field. The results demonstrate that the introduced inversion symmetry breaking affects the nature of superconductivity through the suppression of the Pauli pair-breaking effects.

Heavy fermion materials are a specific type of intermetallic compound consisting of elements with *f* electrons. In these materials, the localized *f* electrons hybridize with the conduction electrons through many-body effects. Hence, the quasiparticle effective mass in strongly enhanced at low temperatures, and sometimes reaches a thousand times the mass of the bare electron. As a result of the competition between itinerant and localized *f* electrons, a plethora of fascinating physical phenomena including unconventional superconductivity with non-*s*-wave pairing symmetry appear in the heavy fermion compounds [1]. The unconventional pairing symmetry and the associated exotic superconducting properties have puzzled and fascinated researchers over the past quarter century.

Recently, the Rashba splitting arising from the inversion symmetry breaking (ISB) has been proposed to affect the superconductivity, giving rise to a variety of novel phenomena such as anomalous magneto-electric effects and topological superconducting states [2]. It has also been suggested that such phenomena are even more pronounced in strongly correlated electron systems [3]. However, the experimental study of the Rashba effect in heavy fermion systems has primarily been performed using bulk single crystals, where the degree of the ISB is hard to be controlled because it is determined by the crystal structure. Therefore, the systematic influence of the ISB on unconventional superconductivity remains an open question.

Here, by using a state-of-the-art molecular beam epitaxy technology, we fabricate a new type of heavy fermion superlattices, i.e. *modulated* superlattices in which the thickness of $CeCoIn_5$ is kept to 5, while the thickness of $YbCoIn_5$ changes between *m* and *m'* from one block layer to the next, forming the *c*-oriented (5:*m*:5:*m'*) superlattices. For the $m \neq m'$ superlattices, the additional ISB along the *c*-axis can be introduced to the superconducting $CeCoIn_5$ block layers. Through the measurements of the temperature and angular dependencies of the upper critical field, we find a significant suppression of the Pauli pair-breaking effect in these superlattices with introducing the ISB. Further we revealed that the magnitude of this suppression increases with the degree of the thickness modulation $|m-m'|$. These results demonstrate that the Rashba spin-orbit interaction in each $CeCoIn_5$ block layer is largely tunable by using the modulated superlattices. Our work paves the way for obtaining novel superconducting states through the thickness modulation in the superlattices with strong spin-orbit coupling [4].

References

[1] C. Pfleiderer, Rev. Mod. Phys. **81,** 1551 (2009).
[2] X. L. Qi and S. C. Zhang, Rev. Mod. Phys. **83,** 1057 (2011).
[3] S. Fujimoto, J. Phys. Soc. Jpn. **76,** 51008 (2007).
[4] M. Shimozawa *et al*., submitted for publication.

Nuclear Magnetic Resonance Studies of Iron Pnictide $BaFe_2(As_{1-x}P_x)_2$

Quantum Materials Laboratory Tetsuya Iye

Abstract We present our nuclear magnetic resonance (NMR) studies of iron-based superconductor (iron pnictide) $BaFe_2(As_{1-x}P_x)_2$. We have clarified quantum criticality, microscopic coexistence and competition between magnetic and superconducting order parameters, and orbital nematicity present in the tetragonal phase of this system.

In this work, we focus on P-underdoped $BaFe_2(As_{1-x}P_x)_2$ showing antiferromagnetic orderings, which are less studied compared to the optimally-doped one. Since the superconductivity appears around the point where antiferromagnetism is suppressed, it is quite important to understand magnetism as the background of the unconventional superconductivity. Static magnetic properties of $BaFe_2(As_{1-x}P_x)_2$ for $0.07 \leq x \leq 0.33$ were investigated by ^{31}P-NMR spectrum measurement. The averaged magnetic ordered moment $\langle m \rangle$ at the zero-temperature limit estimated from the ^{31}P-NMR spectrum shows a continuous suppression toward $x \sim 0.35$ with increasing P concentration x, verifying a second-order quantum phase transition. This result provides evidence of the existence of an antiferromagnetic (AFM) quantum critical point at $x \sim 0.35$, consistent with the normal state properties [1].

The coexisting state of magnetism and superconductivity is one of the most intriguing subject to study since the mechanism of unconventional superconductivity is expected to be highly related to magnetic fluctuation [2]. ^{31}P-NMR measurement on $BaFe_2(As_{1-x}P_x)_2$ for $x = 0.20$ at hydrostatic pressure of $p \sim 2$ GPa was performed. $(T_1T)^{-1}$ measurement on ^{31}P nuclei in the AFM ordered state revealed that an SC transition occurs at the AFM ordered site for $x = 0.20$ ($p \sim 2$ GPa). This is the direct evidence of real-space coexistence of superconductivity and antiferromagnetism in the microscopic scale. Moreover, ^{31}P-NMR spectrum was found to become narrow below T_c, indicative of the suppression of internal magnetic field due to the competition between SC and AFM order parameters. Our results suggest that antiferromagnetism and superconductivity occur at the same Fermi surfaces and compete with each other.

In the recent research field of iron pnictides, the electronic nematic state has been a hot topic in which the electronic state spontaneously breaks the fourfold lattice symmetry in the tetragonal phase thus making various physical properties twofold symmetric in the Fe plane [3]. Motivated by this, we measured in-plane field orientation dependence of ^{75}As-NMR spectrum of single-crystal $BaFe_2(As_{1-x}P_x)_2$ above the structural phase transition temperature T_S. A large difference in the spectral linewidth between $H \parallel [100]_o$ and $H \parallel [110]_o$ in the orthorhombic basis revealed that in-plane anisotropy of the electric field gradient is present even in the tetragonal phase. This in-plane anisotropy arises from population imbalance between As-4p_x and 4p_y orbitals, which reaches $|n_x - n_y| \sim 0.004$ electron at $T \rightarrow T_S$. The orbital polarization is found to be further enhanced below $\sim$ 150 K, which is consistent with the emergence of nematicity in torque and photoemission measurements. This result indicates either a crossover in the magnitude/length of the orbital-nematic correlations, or a phase transition.

References

[1] S. Kasahara *et al.*, Phys. Rev. B **81**, 184519 (2010). Y. Nakai *et al.*, Phys. Rev. Lett. **105**, 107003 (2010). H. Shishido *et al.*, Phys. Rev. Lett. **104**, 057008 (2010).
[2] P. Dai *et al.*, Nature Phys. **8**, 709 (2012).
[3] J.-H. Chu *et al.*, Science **329**, 824 (2010). S. Kasahara *et al.*, Nature **486**, 382 (2012).

Field-induced nematic caps on the colloidal particles

Phase transition dynamics group Takayuki Uchida

Abstract We numerically investigate effects of electric fields in a disordered nematogenic liquid containing dielectric particles. Because of the inhomogeneity of the permittivity, nematic domains are stably formed near the poles of the particle in the electric field. These locally induced nematic domains may change macroscopic properties of the disordered host media. For example, we found Kerr effect of a nematogenic liquid can be drastically enlarged by adding a small amount of dielectric particles. ©*Department of Physics, Kyoto University*

Electrostatic properties of nematic liquid crystals are very important from scientific and industrial viewpoints. In order to calculate a nematic order parameter Q_{ij} under a uniform electric field $\boldsymbol{E}_0$, one usually starts from an electrostatic free energy of the nematic liquid crystal [1],

$$\mathcal{F}_{\rm e} = -\frac{1}{8\pi}\int d\boldsymbol{r}\Big[\varepsilon_0 {E_0}^2 + \varepsilon_1 Q_{ij} E_{0i} E_{0j}\Big], \tag{1}$$

where ε_0 and ε_1 represent isotropic and anisotropic parts of the permittivity, respectively. However, eq.(1) is sometimes inadequate because the electric field is not necessarily uniform. More precisely, the electric field depends on the nematic order parameter. So we should solve the Poisson equation (2) and the following form of the electrostatic free energy (eq.(3)) to obtain the precise electric field $\boldsymbol{E}$ [2,3]:

$$\nabla_i(\varepsilon_{ij}E_j) = 0, \varepsilon_{ij} = \varepsilon_0\delta_{ij} + \varepsilon_1 Q_{ij} + \varepsilon_{\rm p}\delta_{ij}, \tag{2}$$

$$\mathcal{F}'_{\rm e} = \frac{1}{8\pi}\int d\boldsymbol{r}\varepsilon_{ij}E_iE_j. \tag{3}$$

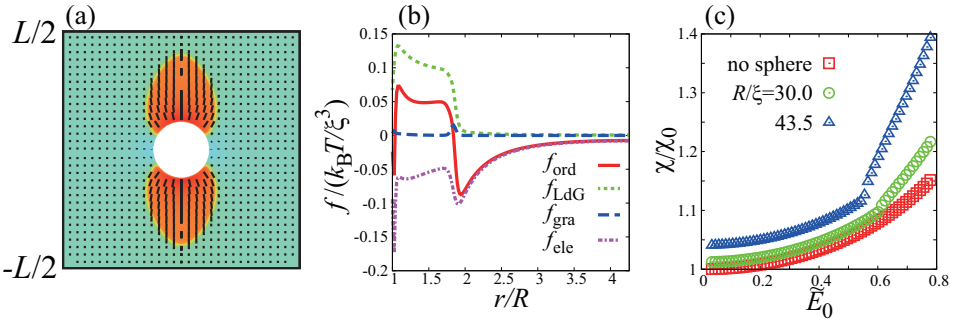

Figure 1: (a) The profile of the nematic order parameter $S = (3Q_{ij}Q_{ji}/2)^{1/2}$ and the director field. (b) The profile of the scaled free energies. (c) The dependence of Kerr coefficient on the external electric field. L: system size, R: sphere radius, ξ: coherent length of the nematogenic liquid, χ_0: Kerr cofficient in the uniform system.

In this work, we study behaviors of a disordered nematogenic liquid containing a spherical colloid. The medium is confined in a capacitor and equilibrated slightly above the isotropic-nematic transition temperature. The dielectric constant of the colloid is assumed to be much larger than that of the host liquid, $\varepsilon_{\rm p} = 20\varepsilon_0$. Then, we impose electric potential differences to the capacitor. We obtain an equilibrium state by numerically minimizing the Landau-de Gennes free energy and eq.(3) with satisfying eq.(2). When the potential difference is sufficiently small, the medium is not ordered as usual. If the potential difference is larger than a threshold, nematic-isotropic transition occurs locally around the poles of the colloid. Although the total free energy density inside the ordered nematic domains is higher than that in the disordered state, the formed nematic-isotropic interfaces are thermodynamically stable (Figure 1a). The formation of the nematic domains is caused by the balance between the ordering free energy $f_{\rm ord}$ inside and outside the nematic domains (Figure 1b). We also found that the induced nematic domains may change macroscopic physical properties of the host disorderd liquid. In Figure 1c, for example, we show a strongly nonlinear increase of the global dielectric constant, or Kerr cofficient, above the transition point.

Reference

[1] P. G. de Gennes and J. Prost, *The Physics of Liquid Crystals* (Clarendon, Oxford, 1993)

[2] A. Onuki, J. Phys. Soc. Jpn **73**, 511 (2004)

[3] K. Tojo, A. Furukawa, T. Araki and A. Onuki, Eur. Phys. J. E **30**, 55 (2009)

Real-Time Detection of Transient Current Induced by Femtosecond Pulse Excitation in Topological Insulators

Solid State Spectroscopy Group Yoshito Onishi

Abstract We have observed terahertz emission from three-dimensional topological insulators under illumination of the femtosecond pulse. The terahertz emission depends on the helicity of the excitation pulse and the crystal-angle, indicating that the origin should be the surface current. A plausible candidate for the surface current would be Floquet-Bloch state formation.

In three-dimensional topological insulators (TIs), nontrivial topology in the bulk insulating state results in the surface electronic state following the massless Dirac equation and the spin state locked by the momentum direction. Optically excited Dirac fermions provide us a good platform to study the non-equilibrium dynamics of relativistic particles interacting with electromagnetic field. Theoretical reports show that spin-selective excitation by circularly polarized light induces asymmetrical distribution in ***k***-space and drives macroscopic current [1]. Actually, current driven by circularly polarized light has been measured with two-terminal sensing [2]. However symmetry breaking by an attachment of electrodes hinders understanding the driving mechanism. In addition, time-resolved techniques are awaited to study transient dynamics of the induced surface current.

In this study, we have investigated transient dynamics of the photo-induced current with a contactless measurement in three-dimensional TIs $Bi_{2-x}Sb_xTe_{3-y}Se_y$ ((x, y) = (0.5, 1.3) and (1, 2)). The current induced by femtosecond pulse emits the electromagnetic wave in terahertz (THz) range. Here we have observed electromagnetic emission proportional to time-derivative of the current driven by a femtosecond near-infrared circularly polarized pulse (pulse width: 100 fs). Fig. 1(a) and (b) show horizontal (a) and vertical (b) components of the emitted THz waveform from $Bi_{1.5}Sb_{0.5}Te_{1.7}Se_{1.3}$ at azimuthal angle θ = 0 degree under the right- or left-handed circularly polarized illumination, respectively. The emitted wave is horizontally polarized and the signs of electric field are opposite between the right- and left- handed circularly polarized excitation. In contrast, at azimuthal angle θ = -30 degrees the THz emission is vertically polarized shown in Fig. 1 (c) and (d). Detailed azimuthal angle dependence of the THz polarization indicates that the polarization rotates synchronized with the rotation of crystal with three-fold rotational symmetry, which is inconsistent with the conventional photogalvanic mechanism for driving photocurrent [2]. Analysis of waveform in time-domain makes it clear that lifetime of current is less than pulse width of excitation pulse.

To account for our experimental results, we propose a new mechanism of driving photocurrent. Light irradiation effectively modifies the electron band structures through virtual photon absorption processes. In this photon-dressed state, called Floquet-Bloch state, light can induce asymmetrically deformed band structure and induce macroscopic current, which we have numerically calculated. The good agreement between experimental and numerical results suggests that photocurrent on the surface would be induced in non-equilibrium steady state where Dirac fermions are hybridized with an applied light field.

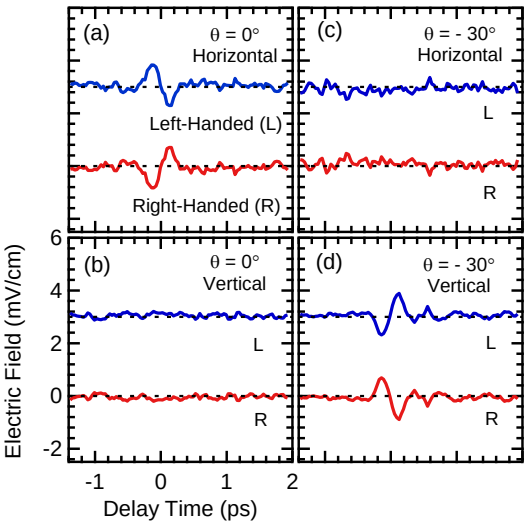

Fig.1 (a)-(d) Time-resolved waveforms emitted from topological insulator $Bi_{1.5}Sb_{0.5}Te_{1.7}Se_{1.3}$ at azimuthal angle θ = 0 (a,b) and θ = -30 degrees (c,d).

References

[1] P. Hosur, Physical Review B **83**, (2011).
[2] J. W. McIver, D. Hsieh, H. Steinberg, P. Jarillo-Herrero, and N. Gedik, Nature Nanotechnology **7**, 96 (2011).

Molecular Dynamics Simulations of Nanobubbles on Substrates

Fluid Physics Group　Shunsuke Kohno

Abstract We performed molecular dynamics simulations of shrinking process of nanobubbles on hydrophobic and hydrophilic substrates in three component Lennard-Jones systems and investigated lifetime of nanobubbles. In the preparation of nanobubbles, we observed semi-cylindrical shaped bubbles due to finite-size effects.

Nanobubbles, which are considered to be one cause of characteristic behavior of fluids in microscopic systems, have been extensively investigated in the past decades. Although their lifetime is theoretically estimated to be an order of μs with a simple diffusion model, the lifetime observed in experiments on the hydrophobic surfaces reaches to a few days. To explain this astonishingly long lifetime of nanobubbles, many mechanisms have been proposed. However, no one turned out to be a dominant cause of their stability. Recently, Lohse et al. proposed a new dynamic equilibrium model, in which the substrate plays an imporant role. However, the origin of re-entrance motions of gas atoms is not clear.[1]

To investigate effects of the substrate to the lifetime of nanobubbles, we performed MD simulations of the shrinking process of nanobubbles in three component Lennard-Jones systems. Periodic boundary conditions are applied to the calculation box. Simulations consist of two steps. In the first step, the temperature of systems is controlled to the one under which nanobubbles are sustained stably in the finite-sized calculation box. At the beginning of the second step, the temperature is suddenly raised to the one under which steady nanobubbles cannot be created spontaneously, and nanobubbles begin to shrink immediately.

In the shrinking process of nanobubbles, the densities of liquid and gas atoms approach to the steady values as shown in Fig.1. Nanobubbles on the substrate shrink relatively slowly compared with those surrounded by the bulk liquid. On the other hand, there is no remarkable difference between the lifetimes of nanobubbles on the hydrophobic and hydrophilic substrates.

In the first step, spherical-cap shaped nanobubbles are created on the hydrophilic substrate, and semi-cylindrical shaped nanobubbles are created on the hydrophobic substrate. When the hydrophobicity is decreased from the hydrophobic state to the hydrophilic state, a semi-cylindrical bubble does not change its shape. On the other hand, increasing the hydrophobicity from the hydrophilic state to the hydrophobic state, a spherical-cap shaped bubble changes its shape to semi-cylindrical at a certain hydrophobicity. Reducing relative bubble volume, a spherical-cap shaped nanobubble changes its shape at higher hydrophobicity. This strongly suggests that semi-cylindrical shaped bubbles are created due to finite-size effects.

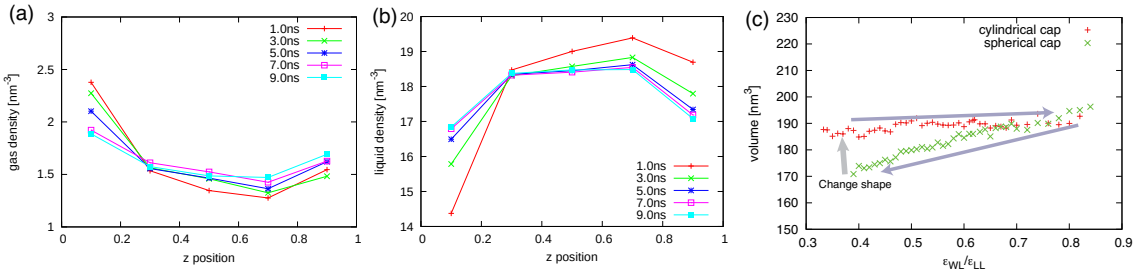

Fig.1　(a) and (b): an example of time evolution of gas and liquid densities outside the bubble averaged in 5 layers perpendicular to the wall. The hydrophobicity is controlled by $\varepsilon_{WL}/\varepsilon_{LL}$(W and L denote wall and liquid, and ε is an strength of LJ interaction.). (c): the volumes of semi-cylindrical and spherical-cap shaped bubbles for various hydrophobicity.

References

[1] J.R.T.Seddon, D.Lohse, W.A.Ducker and V.S.J.Craig, Chemphyschem. **13**, 2179 (2012)

Studying Spatial Distribution of Order Parameter in Superfluid ^{3}He with Nuclear Magnetic Resonance Imaging

Low Temperature Physics Laboratory Masatomo Kanemoto

Abstract Resonance frequency of NMR in superfluid ^{3}He reflects the local orientation of internal degree of freedom of the order parameter. I developed *a* method to measure the spatial distribution of the resonance frequency in order to study inhomogeneous order parameter in superfluid ^{3}He.

2014 Department of Physics, Kyoto University

Superfluid ^{3}He is a p-wave pair condensate with multiple internal degrees of freedom. So superfluid ^{3}He has multiple phases. In the A-phase, the order parameter is expressed by two vectors, ***d*** and ***l***. In the B-phase, the order parameter is expressed by ***n*** vector and a rotation angle θ. Order parameter may vary in space. The spatial distribution of the order parameter is called as a texture. The texture is determined by minimizing the sum of various energies. Dipole energy is the energy due to the dipole interaction acting on two spins which make pair. Gradient energy comes from the spatial variation of the order parameter. Magnetic energy originates from the anisotropy in magnetic susceptibility. In addition, pair breaking effect near the boundary orients orbital angular momentum of the pair to be perpendicular to the walls of the container.

An NMR signal in superfluid ^{3}He is characterized by a frequency shift from Larmor frequency which is determined by applied magnetic field. The frequency shift varies in space because of the texture. For example, in the A-phase, ***d*** and ***l*** orient parallel or anti-parallel with each other due to the dipole interaction. If there are parallel and anti-parallel domains there appears a region where ***d*** and/or ***l*** rotate gradually in space in order to connect order parameters on each sides. This region is called as a domain wall. A frequency shift at the domain wall is reduced compared to that from the bulk part. The existence of the domain wall is proven by NMR satellite peak in the spectrum. However the actual shape of the domain wall in real space is not clearly studied. In the B-phase magnon BEC was observed at very low temperature. The observed irregular decay of the magnon BEC suggested the presence of the domain wall as well. A phase boundary between the A-phase and the B-phase can be stabilized under magnetic field gradient. The texture near the phase boundary is not yet clearly understood. Thus a new method to directly measure the shape of the texture in space is strongly awaited.

In standard MRI the spatial distribution is mapped onto the distribution of resonant frequency by applying a magnetic field gradient. In the case of superfluid ^{3}He, it is impossible to obtain the image by this method because we can not distinguish the frequency shift and the effect of applied magnetic field gradient. Therefore, we developed a new technique called Magnetic Resonance Spectroscopic Imaging (MRSI). In MRSI, we obtain a set of NMR signals with various intensity of the magnetic field gradient *G* with identical direction. Then we can extract spatial distributions by Fourier transformation in *G* and then the frequency distributions by Fourier transformation in time. The MRSI can be the first tool to study inhomogeneous texture.

As the first practical test of the MRSI, we did the experiment with liquid ^{3}He in a parallel plate cell whose gap was 100 micrometer. Figure 1 shows the measured frequency distribution in the normal phase under an intensionally applied linear magnetic field gradient. Residual magnetic field distribution after canceling linear field gradients in X,Y,Z directions is shown in Fig. 2. The saddle shaped distribution was consistent with the quadratic magnetic field distribution. Spatially integrated frequency distribution was in good agreement with the standard NMR spectrum. MRSI measurement in the A-phase showed uniform frequency shift as expected in the parallel plate cell. Thus I could prove that MRSI measurement is applicable to the superfluid state.

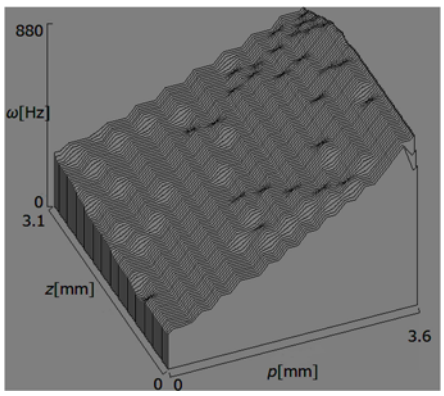

Fig.1. Measured frequency distribution ω in a parallel plate cell under linear field gradient along *p* axis.

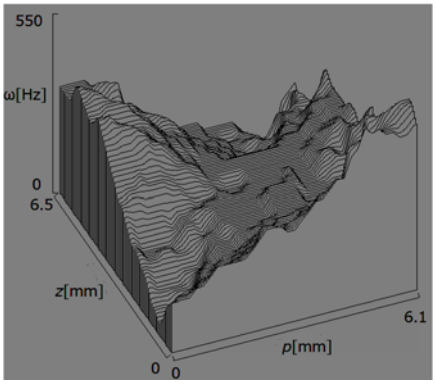

Fig.2. Quadratic field distribution after canceling linear fiel

Mode bifurcation of droplet motion under stationary laser irradiation

Dissipative Structure and Biological Physics Fumi Takabatake

Abstract Self-propelled motion of an oil droplet induced by a local temperature gradient under laser irradiation is investigated. With an increase in the laser power, droplet motion transitions from rectilinear motion to rotary motion. This mode bifurcation is interpreted in terms of spontaneous symmetry-breaking depending on the energy flux rate.

Inhomogeneous temperature and/or chemical concentration at the interface generate tangential flow along the interface, which is called Marangoni flow. When Marangoni flow is induced at a free fluid interface, self-propelled motions of the objects floating on the interface are generated by their interfacial tension gradient. Such self-propelled object exhibits irregular motion called active Brownian motion under isotropic boundary conditions. In contrast, by selecting a suitable boundary condition, e.g., internal or external asymmetry, it becomes possible to extract regular motion with a specific mode according to its symmetry [1]. Furthermore, we recently reported that self-propelled motion can undergo mode bifurcation depending on the degree of non-equilibrium through spontaneous symmetry-breaking, even under boundary conditions with the same symmetry [2].

In order to verify the spontaneous mode bifurcation, we investigated a self-propelled motion of a mm-sized droplet floating on water driven by local heating with a spatially-fixed laser. The motion of the oil droplet is induced through the generation of shear flow due to interfacial tension gradient, i.e., thermal Marangoni convection. It was found that the mode of the motion of the circular droplet bifurcates into qualitatively different types of regular motion, i.e., rectilinear reciprocal motion and circular orbital motion, with an increase in the heating power (Fig. 1). The essential features of this mode-bifurcation are discussed in terms of spontaneous symmetry-breaking under a high gradient of temperature, and are reproduced with simple ordinary differential equations by incorporating a delay function of the Marangoni convection and heated position.

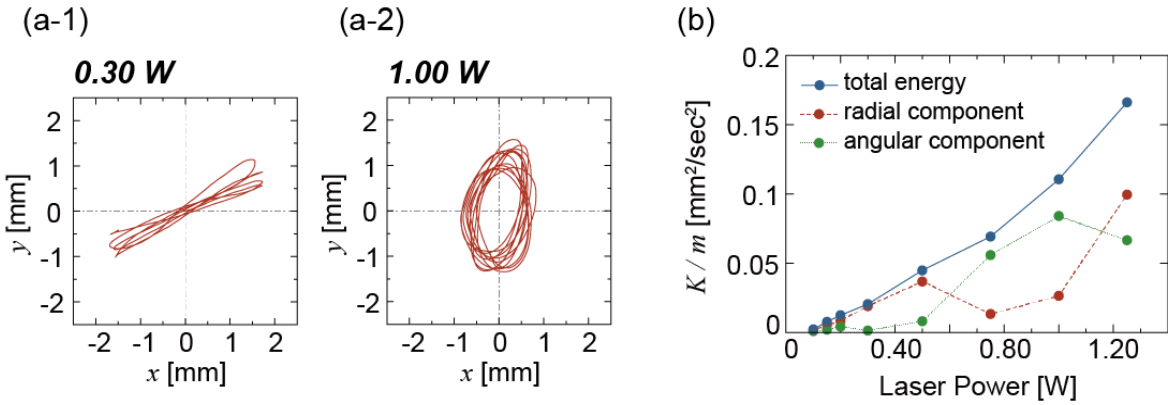

Fig. 1. (a) Trajectories of the center of the droplet. The mode of droplet motion changes from rectilinear reciprocal motion to circular motion. The laser power was (a-1) 0.30 mW and (a-2) 1.00 mW. The volume of the droplet was 20 μl. (b) The variation in translational kinetic energy per unit mass with respect to the laser power.

References

[1] S. Nakata, Y. Iguchi, S. Ose, M. Kuboyama, T. Ishii, and K. Yoshikawa, *Langmuir* **13**, 4454 (1997).
[2] F. Takabatake, N. Magome, M. Ichikawa, and K. Yoshikawa, *J. Chem. Phys.* **134**, 114704 (2011).

In-plane anisotropy of the uniaxial pressure effect on the Mott insulator Ca_2RuO_4

Quantum Materials Lab. Haruka TANIGUCHI

Abstract The antiferromagnetic Mott insulator Ca_2RuO_4 exhibits various electronic states depending on lattice distortions through strong coupling between the lattice and orbital degrees of freedom. By in-plane uniaxial pressures, we newly induced ferromagnetic metallic phase. Furthermore, we revealed substantial anisotropy in the uniaxial-pressure response. We discuss the origin of these phenomena.

The antiferromagnetic Mott insulator Ca_2RuO_4 exhibits drastic changes in its electronic states under external stimuli such as isovalent Sr-Ca substitution, hydrostatic pressure, epitaxial stress in thin film, or electric field [1]. Such changes are caused because the orbital degree of freedom strongly couples with the lattice distortion. For example, it has been known that ferromagnetic metallic (FM-M) phase emerges when the RuO_6 octahedra in the structure are elongated along the *c* axis [2]. Thus, we aimed to control the electronic state of Ca_2RuO_4, by using in-plane uniaxial pressures, which stretch the lattice along the *c* axis more effectively. We measured the electric resistance and magnetization under in-plane uniaxial pressures with two different pressure directions: parallel and diagonal to the in-plane Ru-O bond of the RuO_6 octahedra (we denote these directions as $[100]_T$ and $[110]_T$, respectively, using the tetragonal notation) [3]. We note that because of the orthorhombic distortion, twin domains are formed with the twin boundaries running along the $[100]_T$ direction.

We succeeded in inducing the FM-M phase with in-plane uniaxial pressures. The critical pressures of the FM-M phase for the uniaxial pressure (0.4 GPa for $P//[100]_T$ and 0.2 GPa for $P//[110]_T$) are substantially lower than that for the hydrostatic pressure (0.5 GPa). This fact demonstrates the effectiveness of the uniaxial pressure to control the electronic state in Ca_2RuO_4. Interestingly, the critical pressures of the FM-M state were found to be highly anisotropic: the critical pressure for $P//[110]_T$ is only a half of that for $P//[100]_T$. In addition, the pressure dependence of the magnetization is also quite anisotropic as shown in Fig.1; In particular, under $P//[110]_T$, the development of the FM component of the magnetization occurs twice from 0.2 to 0.4 GPa and above 1.2 GPa. These peculiar anisotropic results can be naturally understood as a consequence of the orthorhombic crystal distortions in Ca_2RuO_4 and existence of orthorhombic crystalline twin domains in the sample.

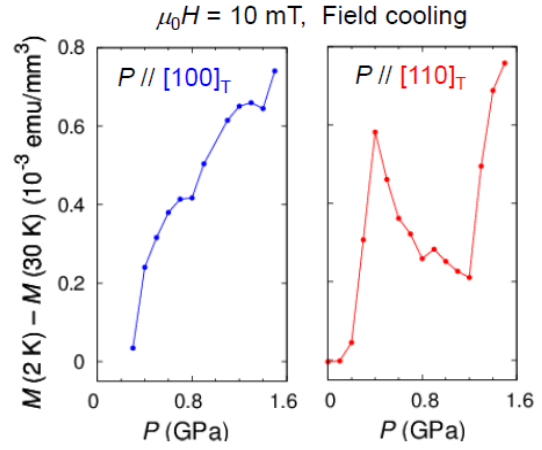

Fig.1. Pressure dependence of ferromagnetic component of magnetization for Ca_2RuO_4 under in-plane uniaxial pressures along the $[100]_T$ or $[110]_T$ directions [3].

References

[1] S. Nakatsuji *et al.*, Phys. Rev. B **62**, 6458 (2000); P. Alireza *et al.*, J. Phys.: Condens. Matter **22**, 052202 (2010); X. Wang *et al.*, Appl. Phys. Lett. **85**, 6146 (2004); F. Nakamura *et al.*, Sci. Rep. **3**, 2536 (2013).
[2] O. Friedt *et al.*, Phys. Rev. B **63**, 174432 (2001); P. Steffens *et al.*, Phys. Rev. B **72**, 094104 (2005).
[3] H. Taniguchi *et al.*, Phys. Rev. B **88**, 205111 (2013).

Study of the electronic states in heavy fermion compound URu_2Si_2

Electronic properties of solids laboratory Sho Tonegawa

Abstract We perform cyclotron resonance and high-resolution synchrotron X-ray experiments in the “hidden order” phase of URu_2Si_2. Our results reveal that the Fermi surface breaks the crystal four-fold symmetry and tiny orthorhombic lattice distortion sets in below the transition. This places strong constraints on the symmetry of the hidden order parameter.

The heavy fermion compound URu_2Si_2 exhibits a second order phase transition at 17.5 K accompanying a huge amount of entropy loss, but no structural and magnetic ordering have been observed. Despite considerable experimental and theoretical efforts for more than a quarter century, the order parameter is not yet totally understood and therefore the phase is called “hidden order” phase. In general, a second-order phase transition causes a change in various types of symmetries, such as rotational, gauge and time reversal symmetries. Therefore the experimental determination of broken symmetries is the most essential step toward elucidating the nature of the hidden order phase transition. Recent magnetic torque and NMR measurements reveal the in-plane anisotropy of magnetic susceptibility [1,2], which suggests that the crystal four-fold rotational symmetry in the tetragonal URu_2Si_2 is broken below the hidden order transition. This newly suggested rotational symmetry broken state (“nematic” state) has raised several theoretical proposals, and calls for further experimental verifications by using other techniques.

For the understanding of the nature of the “nematic” state, it is important to clarify how the electronic structure is related to the rotational symmetry breaking. We therefore perform cyclotron resonance measurements in the hidden order phase, which allow the full determination of angle-dependent electron-mass structure of the main Fermi-surface sheets. Furthermore, we find an anomalous splitting of the sharpest resonance line under in-plane magnetic-field rotation. This is most naturally explained by the domain formation, which breaks the fourfold rotational symmetry of the underlying tetragonal lattice. The results reveal the emergence of an in-plane mass anisotropy with hot spots along the [110] direction, which indicates that the Fermi surface breaks the four-fold rotational symmetry in the hidden order phase [3,4].

Another important aspect of the “nematic” state is whether the rotational symmetry breaking is induced by external magnetic field, because the torque, NMR and cyclotron resonance experiments have been carried out under in-plane magnetic field [1-4]. We therefore perform high-resolution synchrotron X-ray crystal-structure analysis at zero field for a high-angle (880) Bragg diffraction by four-circle diffractometer. We find tiny but finite orthorhombic distortion of the order of 10^{-5} (or lattice constant change less than 100 fm), which suggests the four-fold rotational symmetry is broken in the absence of magnetic field [5].

References

[1] R. Okazaki *et al*., Science **331**, 439 (2011).
[2] S. Kambe *et al*., Physical Review Letters **110**, 246406 (2013).
[3] S. Tonegawa *et al*., Physical Review Letters **109**, 036401(2012).
[4] S. Tonegawa *et al*., Physical Review B (in press).
[5] S. Tonegawa *et al*., submitted for publication.

Antiferromagnetic ordering induced by paramagnetic pair-breaking in strong-coupling superconducting states

Condensed matter theory group　　Yuhki Hatakeyama

Abstract We investigate the two-dimensional Hubbard model including the Zeeman energy with the fluctuation-exchange (FLEX) approximation in order to discuss antiferromagnetic ordering induced by paramagnetic pair-breaking (PPB) in strong-coupling superconductors. We also examine the influence of the strong-coupling effects on the PPB-induced antiferromagnetic ordering.

Recently, field-induced enhancement of antiferromagnetism in d-wave superconductors with a strong paramagnetic pair-breaking (PPB) effect have been observed. In the high-field low-temperature (HFLT) phase of $CeCoIn_5$, an antiferromagnetic (AFM) order coexists with a Fulde-Ferrell-Larkin-Ovchinnikov (FFLO) superconducting (SC) order and is present only in the HFLT phase[1]. An AFM order existing near the SC transition field $H_{c2}(0)$ is also observed in pressurized $CeRhIn_5$[2]. Moreover, a field-induced AFM quantum critical point (QCP) located slightly below $H_{c2}(0)$ is suggested in many d-wave superconductors with a strong PPB effect.

Our previous study based on the weak-coupling BCS model[3] has shown that, in the high-field region of a d-wave SC phase with strong PPB, an AFM order can be realized more easily than in the normal state. The above observations can be explained on the basis of this mechanism. However, a SC state with strong PPB tends to be realized in materials with a strong electron correlation and an AFM fluctuation, which are not incorporated in the weak-coupling BCS model, and these effects can affect the PPB-induced AFM ordering. Consequently, it is necessary to extend the theory of the PPB-induced AFM ordering to the case of strong-coupling SC states.

In this study, we discuss the PPB-induced AFM ordering in strong-coupling SC states by investigating the two-dimensional Hubbard model including the Zeeman energy using the fluctuation-exchange (FLEX) approximation[4]. On the basis of the calculation of the transverse AFM susceptibility, we show that the PPB-induced AFM ordering is realized in strong-coupling SC states through the mechanism similar to that in the weak-coupling model. We also show that the PPB-induced AFM ordering is affected chiefly by the following three strong-coupling effects: the quasiparticle renormalization (i.e. the mass enhancement), the amplitude of the SC order parameter, and the Stoner enhancement in the normal state. We find that promotion of the PPB-induced AFM ordering owing to the Stoner enhancement dominate over the other two effects in the situation close to an AFM-QCP. Therefore, an AFM order existing only in the high-field region of the SC phase is expected to be realized in d-wave superconductors with a strong PPB effect close to an AFM-QCP.

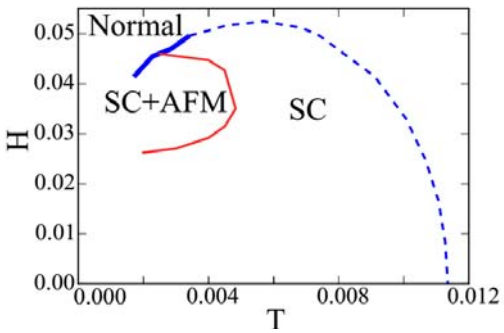

Fig. 1. H-T phase diagram obtained from the numerical calculation in the strong-coupling model

References

[1] K. Kumagai *et al.*, Phys. Rev. Lett. **106**, 137004 (2011).
[2] T. Park *et al.*, Nature **440**, 65 (2006).
[3] R. Ikeda *et al.*, Phys. Rev. B **82**, 060510 (2010); Y. Hatakeyama and R. Ikeda, Phys. Rev. B **83**, 224518 (2011).
[4] Y. Hatakeyama and R. Ikeda, arXiv:1309.4609 (to be published in J. Phys. Soc. Jpn.).

Spin-Triplet Superconductivity Induced by Ferromagnetic Fluctuations in UCoGe

Quantum Materials Lab. Taisuke HATTORI

Abstract We have investigated the relationship between ferromagnetism and superconductivity with using NMR measurements on the ferromagnetic superconductor UCoGe. Our experimental results strongly suggest that longitudinal ferromagnetic fluctuations play an important role for a pairing mechanism of the spin-triplet superconductivity in UCoGe.

Identification of pairing mechanism leading to the unconventional superconductivity is one of the most challenging issues in condensed-matter physics. Therefore the discovery of superconductivity in the ferromagnet UGe_2 under pressure in 2000 had a great impact since we can investigate the relationship between ferromagnetic (FM) fluctuations and superconductivity. So far, four uranium FM superconductors have been reported: UGe_2, URhGe, UIr, and UCoGe.

In these FM superconductors, UCoGe is one of the most experimentally explored, because of the highest superconducting (SC) transition temperature T_{SC} ~ 0.8 K and lowest Curie temperature T_{Curie} ~ 3 K at ambient pressure[1]. To clarify the relationship between ferromagnetism and superconductivity, we have performed nuclear quadrupole resonance (NQR) / nuclear magnetic resonance (NMR) measurements on UCoGe. We have shown that superconductivity occurs within the FM region, resulting in the microscopic coexistence of ferromagnetism and superconductivity[2]. Although the crystal structure is three dimensional, magnetic properties possess strong Ising anisotropy with the *c* axis being the easy axis[3]. In addition, it is reported that the SC upper critical limiting field H_{c2} has also large anisotropy[3,4]: superconductivity survives with the external field as large as 15 T along the *a* and *b* axes, whereas along the *c* axis is as small as 0.5 T. This large H_{c2} along the *a* axis is suppressed with a steep angle dependence when the field was tilted slightly from the *a* axis toward the *c* axis[4]. The observed characteristic H_{c2} behavior is one of the mysterious features of the superconductivity of UCoGe, and its origin would be related to the mechanism of the superconductivity.

From the angle-resolved NMR measurements we showed that longitudinal FM fluctuations along the *c* axis are dominant in UCoGe[5]. In addition, we found that these longitudinal FM fluctuations are well tuned by the external magnetic field: the magnetic field along the *c* axis $H \parallel c$ suppresses the fluctuations drastically[6]. Interestingly these tunable FM fluctuations seem to be related to the superconductivity since the anisotropy of the FM fluctuations is well scaled to that of the superconductivity (Fig. 1[6]). Combined with the theoretical model calculation, the longitudinal FM fluctuations are strongly suggested to be a SC pairing glue, concomitantly resolving the above-mentioned puzzle of H_{c2}.

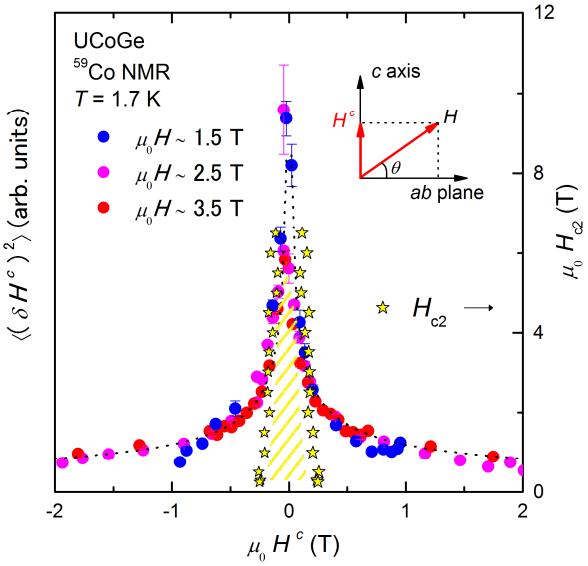

Fig.1 H^c dependence of magnetic fluctuations along the *c* axis $\langle(\delta H^c)^2\rangle$ at 1.7 K. H_{c2} is also plotted against H^c.

References

[1] N. T. Huy *et al.*, *Phys. Rev. Lett.* **99**, 067006 (2007).
[2] T. Ohta *et al.*, *J. Phys. Soc. Jpn.* **79**, 023707 (2010).
[3] N. T. Huy *et al.*, *Phys. Rev. Lett.* **100**, 077002 (2008).
[4] D. Aoki *et al.*, *J. Phys. Soc. Jpn.* **78**, 113709 (2009).
[5] Y. Ihara *et al.*, *Phys. Rev. Lett.* **105**, 206403 (2010).
[6] T. Hattori *et al.*, *Phys. Rev. Lett.* **108**, 066403 (2012).

Structural and dynamical studies on the supra-protein complex in an active state

Biological Molecular Structure Group　　Yuya Morita

Abstract The 26S proteasome is a huge molecular machine that degrades unnecessary proteins in the living cell. We focused the catalytic domains of the 26S during the degradation process, and found that 26S has an exporting mechanism of the degraded peptides.

The 26S proteasome is a ~2.5MDa molecular machine, and degrades unnecessary proteins at a metabolic turnover in the living cell. It is composed of a barrel-shaped 20S core particle (CP) that is capped on both ends by 19S regulatory particle (RP). 20S is formed by axial stacking of four heptameric rings: 2 inner beta-rings and 2 outer alpha-rings. There are 3 active sites between 2 beta-rings, and 20S can degrade proteins when 1 or 2 alpha-rings of 20S are capped by 19S. One of the main questions is what occurs in the 26S conformational change during the degradation process. There are some reports [1, 2] about 19S “rough” (~10Å) conformational changes by electron microscopy during the degradation process, but there are few reports about 20S “precise” (~2.5 Å)conformational changes as a part of the active 26S . Therefore, we investigated 20S conformational changes between active and inactive states.

We added a detergent, Sodium Dodecyl Sulfate (SDS), to 20S in order to mimic the 20S conformation changes as a part of the 26S at the protein degradation process. This “mimic 20S” structure was analyzed by X-ray crystal structural analysis (resolution: 2.5Å). As a result, some holes on the side of 20S became larger and new beta-strands were produced. These 20S conformational changes indicate that there exists and gives a mechanism in the 26S by which 26S exports unnecessary peptides from the produced side “dust holes”.

In addition, we verified our “dust hole model”, and approximately evaluated the dust hole size of 26S at the degradation process. M. E. Matyskiela et al. [1] pointed out that 19S rotates by intrinsic angles when 26S degrades a substrate. We hypothesized that 26S was twisted by both 19S rotations. We approximated 26S as a cylindrical rigid body, and concluded the gap variation as 3 ± 2Å.

Although there remain some important factors that were not taken into account, such as secondary structures, our “dust hole model” reveals a mechanism that have not been pointed out by electron microscopic structural analysis. In order to discuss our model more precisely, it is necessary to analyze 26S structure at ~2.0Å resolution. We are trying to analyze 26S structure by X-ray structural analysis, and to construct the experimental system to verify the effect of the “19S twist“ to the dust holes.

References

[1] M. E. Matyskiela *et al.*, NATURE STRUCTUAL & MOLECULAR BIOLOGY **20**, 781-788 (2013).
[2] S. Bohn *et al.*, PNAS **107**, 20992-20997 (2010)
[3] R. Beckwith *et al.*, NATURE STRUCTUAL & MOLECULAR BIOLOGY **20**, 1165-1172 (2013)

Phase separation in a binary mixture confined between symmetric parallel plates: Capillary condensation transition near the bulk critical point

Phase Transition Dynamics Group Shunsuke Yabunaka

Abstract We investigate phase separation of near-critical binary mixtures between parallel symmetric walls in the strong adsorption regime. We lower the temperature T below the capillary condensation line from above the capillary critical temperature and investigate the phase separation dynamics. A pancake domain of the phase disfavored by the walls finally appears in the middle of the film.

The phase behavior of fluids confined in narrow regions has been studied extensively. It strongly depends on the geometry of the walls and on the molecular interactions between the fluid and the walls. Its understanding is crucial in the physics of fluids in porous media. It is also needed to study the dynamics of confined fluids. As one of the simplest cases, we study the phase transition dynamics of a binary mixture confined between symmetric parallel plates [1].

We take into account the renormalization effect due to the critical fluctuations using the recent local functional theory [2]. In statics, a van der Waals loop is obtained in the relation between the average order parameter ϕ in the film and the chemical potential when the temperature T is lower than the film critical temperature T_{ca}. In dynamics, we lower T below the capillary condensation line from above T_{ca}, and calculate the subsequent time development assuming no mass exchange between the film and the reservoir. In the early stage, the order parameter ϕ changes only in the direction perpendicular to the walls. For sufficiently deep quenching, such one-dimensional profiles become unstable with respect to the fluctuations varying in the lateral directions. The late-stage coarsening is then accelerated by the hydrodynamic interaction. A pancake domain of the phase disfavored by the walls finally appears in the middle of the film.

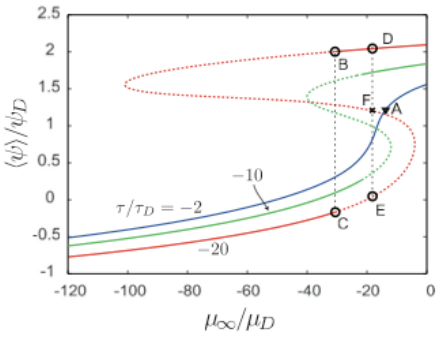

Fig. 1. The chemical potential obtained from the 1D solutions with the average order parameter $<\psi>$.

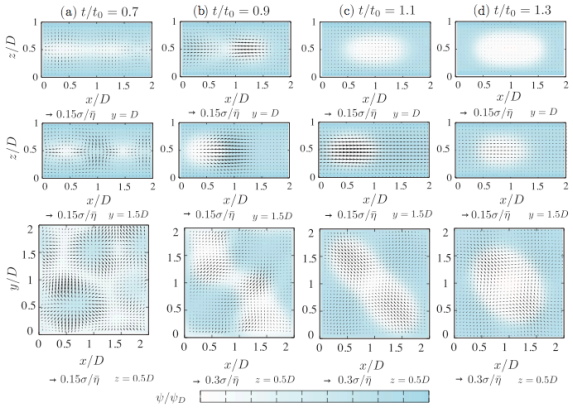

Fig. 2. Cross sectional velocity field $\vec{v}$ and order parameter field ψ in phase separation.

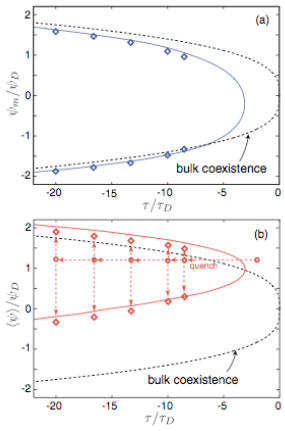

Fig. 3. Phase diagrams in the τ/τ_D - ψ_m/ψ_D plane in (a) and τ/τ_D - $<\psi>/\psi_D$ plane, where ψ_m is the midpoint value.

References

[1] S. Yabunaka, R. Okamoto, and A. Onuki, Phys. Rev. E 87 032405(2013).
[2] R. Okamoto and A. Onuki, J. Chem. Phys. 136, 114704 (2012)

Theoretical study of correlated topological insulators

Condensed matter theory group Tsuneya Yoshida

Abstract After discovery of topological insulators, topological aspects of quantum phases have attracted much interest. One of the current important issues is the correlation effect on these phases. In this study, we address this issue by employing the dynamical mean field theory and the density matrix renormalization group.

In this decade, topological insulators have been found and provided a new arena of study in condensed matter physics. Recently, realizations of nontrivial insulators in *d-, f-* electron systems are proposed (e.g, Na_2IrO_3, SmB_6, LuPtSb, *etc.*), and the correlation effect on topological insulators is one of the current important issues. Motivated by these studies, we address this issue by making use of nonperturbative methods and elucidate the following behaviors.

(i) Mott transition in two-dimensional topological insulators. In the strongly correlated region, Mott insulars, whose origin differs from that of band insulators, are realized. Thus, one can ask how the topological insulator in the weakly correlated systems changes into a Mott insulator. To address this issue, we employ the dynamical mean field theory (DMFT) and the continuous time quantum Monte Carlo method. Interaction dependence of the spin Hall conductivity and the double occupancy reveals that the topological insulator changes into a trivial Mott insulator via a first order transition [1]. This paramagnetic Mott transition is expected to be observed in geometrically frustrated topological insulators such as Pr_2IrO_7.

(ii) Antiferromagnetic topological insulators. It is known that in the single-particle framework, antiferromagnetic insulators can also possess nontrivial structures, but it is unclear if such phases are realized even beyond the Hartree approximation. Our DMFT results clarify that this type of nontrivial magnetic insulators is indeed realized in correlated systems [2].

(iii) Spin-selective topological Kondo insulators. The RKKY and the Kondo effects are source of intriguing behaviors in heavy fermion systems. Recently, even for these systems nontrivial insulators, called topological Kondo insulators, are proposed. In this study, we address how these two essential effects affect topological phases and propose a new type of quantum phases, spin-selective topological Kondo insulators, which are realized in a ferromagnetic *metallic* phase and shows non-Tomonaga-Luttinger liquid behaviors at edges. We expect that this exotic edge behavior can be observed by NMR experiments [3].

(iv) Topological Mott insulators in one dimension. In strongly correlated systems, topological Mott insulators which host gapless spion excitations rather than electron excitations at edges are proposed. Unfortunately, this type of quantum phase has not been established yet, although various numerical analyses tried to find it. Our results obtained by density matrix renormalization group establish realization of this phase in a one-dimensional system with the chiral symmetry. Furthermore, in this system, we observe a topological phase transition without gap-closing in the single-particle excitation spectrum [4].

References

[1] T. Yoshida *et al.,* Phys. Rev. B **85** 125113 (2012).
[2] T. Yoshida *et al.,* Phys. Rev. B **87** 085134 (2013).
[3] T. Yoshida *et al.,* Phys. Rev. B **87** 165109 (2013).
[4] T. Yoshida *et al,* submitted.